Cell Reports
Medicine

Article

A comprehensive analysis and resource to use CRISPR-Cas13 for broad-spectrum targeting of RNA viruses

Graphical abstract

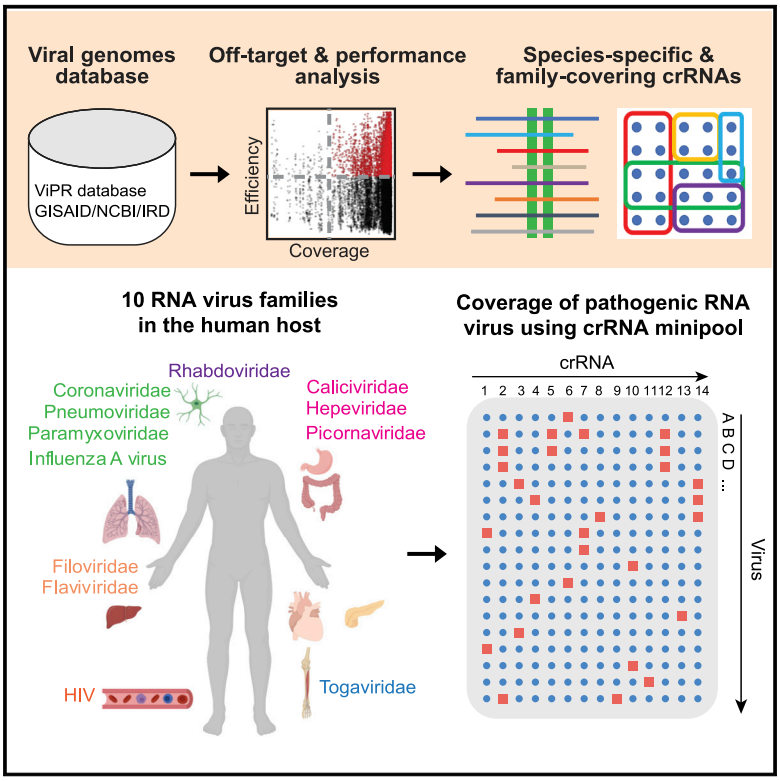

Highlights

- A web resource for using CRISPR-Cas13 to target broad RNA virus families
- A bioinformatic tool to analyze efficiency and specificity of virus-targeting crRNAs
- A minipool of crRNAs can target 90% of human-infectious RNA viruses
- Validated crRNAs are predicted to target newly emerging SARS-CoV-2 variants

Authors

Xueqiu Lin, Yanxia Liu, Augustine Chemparathy, Tara Pande, Marie La Russa, Lei S. Qi

Correspondence

stanley.qi@stanford.edu

In brief

Lin et al. develop a bioinformatic tool and an online resource for using CRISPR-Cas13 to target diverse human-infecting RNA viruses (10 families and 24,096 strains) with high efficiency and specificity.

Lin et al., 2021, Cell Reports Medicine 2, 100245
April 20, 2021
https://doi.org/10.1016/j.xcrm.2021.100245

CellPress

Cell Reports Medicine

CellPress
OPEN ACCESS

Article

A comprehensive analysis and resource to use CRISPR-Cas13 for broad-spectrum targeting of RNA viruses

Xueqiu Lin,[1,6] Yanxia Liu,[1,6,7] Augustine Chemparathy,[1,2,6] Tara Pande,[3] Marie La Russa,[1,7] and Lei S. Qi[1,4,5,7,8,*]
[1]Department of Bioengineering, Stanford University, Stanford, CA 94305, USA
[2]Department of Management Science and Engineering, Stanford University, Stanford, CA 94305, USA
[3]Los Altos High School, Los Altos, CA 94022, USA
[4]Department of Chemical and Systems Biology, Stanford University, Stanford, CA 94305, USA
[5]ChEM-H, Stanford University, Stanford, CA 94305, USA
[6]These authors contributed equally
[7]Senior author
[8]Lead contact
*Correspondence: stanley.qi@stanford.edu
https://doi.org/10.1016/j.xcrm.2021.100245

SUMMARY

The coronavirus disease 2019 (COVID-19) pandemic caused by severe acute respiratory syndrome-coronavirus-2 (SARS-CoV-2) and variants has led to significant mortality. We recently reported that an RNA-targeting CRISPR-Cas13 system, called prophylactic antiviral CRISPR in human cells (PAC-MAN), offered an antiviral strategy against SARS-CoV-2 and influenza A virus. Here, we expand *in silico* analysis to use PAC-MAN to target a broad spectrum of human- or livestock-infectious RNA viruses with high specificity, coverage, and predicted efficiency. Our analysis reveals that a minimal set of 14 CRISPR RNAs (crRNAs) is able to target >90% of human-infectious viruses across 10 RNA virus families. We predict that a set of 5 experimentally validated crRNAs can target new SARS-CoV-2 variant sequences with zero mismatches. We also build an online resource (crispr-pacman.stanford.edu) to support community use of CRISPR-Cas13 for broad-spectrum RNA virus targeting. Our work provides a new bioinformatic resource for using CRISPR-Cas13 to target diverse RNA viruses to facilitate the development of CRISPR-based antivirals.

INTRODUCTION

Since December 2019, the world has been devastated by the coronavirus disease 2019 (COVID-19) pandemic caused by the RNA virus severe acute respiratory syndrome-coronavirus-2 (SARS-CoV-2). In addition to SARS-CoV-2, the outbreaks of RNA viruses in recent years, including Zika virus, Ebola virus, Marburg virus, and MERS (Middle East respiratory syndrome) virus, have led the World Health Organization (WHO) to declare public health emergencies. While vaccines and therapeutic options against SARS-CoV-2 have advanced into clinical trials, most RNA viruses lack an approved therapy.[1]

In search of potential antivirals, we recently developed a CRISPR-Cas13d-based strategy, PAC-MAN (prophylactic antiviral CRISPR in human cells) to target and inhibit SARS-CoV-2 and influenza A virus (IAV) sequences.[2] A few researchers also reported that CRISPR-Cas13a/b systems can be used to inhibit RNA viruses, including lymphocytic choriomeningitis virus (LCMV), vesicular stomatitis virus (VSV), human immunodeficiency virus type 1 (HIV-1), human respiratory syncytial virus (HRSV), Dengue virus, Turnip mosaic virus, and tobacco turnip mosaic RNA virus (TuMV).[3–9] The CRISPR-Cas13 systems (subtypes a, b, and d) offer attractive prophylactic or therapeutic options due to 2 key features: (1) CRISPR-Cas13 is highly programmable, which allows it to be rapidly adapted against new RNA viruses by designing the CRISPR RNA (crRNA) sequence[5,9] and (2) crRNAs can be designed to target highly conserved viral sequences to cover multiple strains and prevent viral mutational escape.[10] One remaining question is whether the system can be expanded to target a broad spectrum of RNA viruses.

Here, we perform a comprehensive *in silico* analysis using PAC-MAN to target notable pathogenic viral species and human-infectious RNA viruses in the Virus Pathogen Database and Analysis Resource (ViPR).[11] We generated an integrated crRNA analysis pipeline by incorporating existing algorithms to compute the coverage, efficiency, and specificity of crRNAs for targeting RNA viruses. Using this pipeline, we identified crRNAs for targeting 16 distinct RNA virus families. We also observed that a minimal set of 14 crRNAs can collectively target >90% of human-infectious strains across 10 non-segmented RNA virus families. For several families of viruses, >90% of sequenced human-infectious strains in the family can be targeted by as few as 1 or 2 crRNAs. In contrast, families of viruses with segmented RNA genomes generally required more

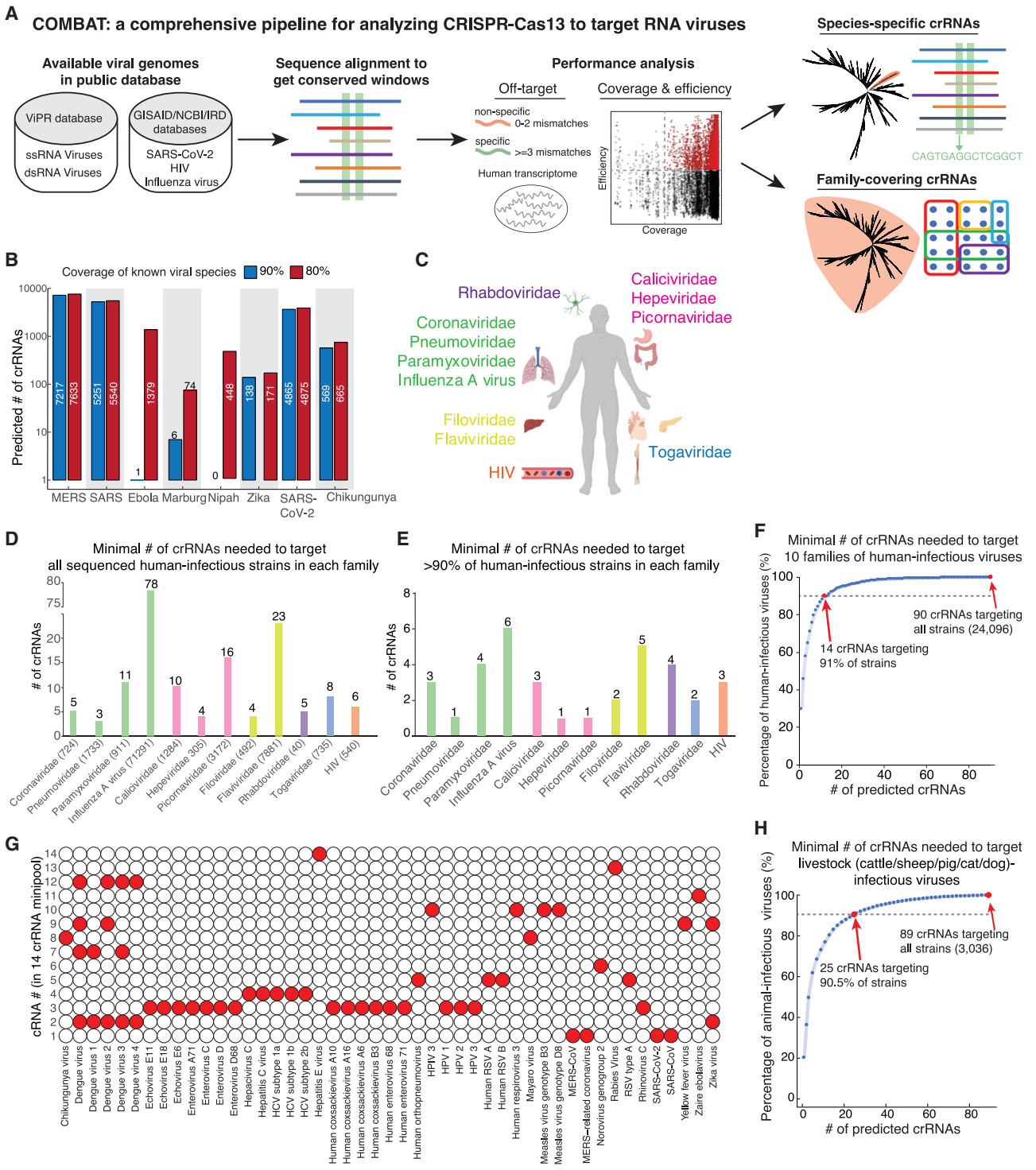

Figure 1. Analysis of PAC-MAN for targeting broad-spectrum RNA viruses

(A) An integrated pipeline for Cas13 crRNA analysis for virus-targeting coverage, efficiency, and specificity.

(B) Targeting pandemic/epidemic-causing pathogenic RNA virus species using PAC-MAN.

(C) Schematic of 10 RNA virus families that target different organs and systems in the human host.

(D) The minimal number of crRNAs needed to target all sequenced human-infectious strains in each of 10 RNA virus families and HIV and IAV.

(E) The minimal number of crRNAs needed to target 90% of sequenced human-infectious strains in each of 10 RNA virus families and HIV and IAV.

(legend continued on next page)

crRNAs for full targeting. We built an online resource (http://crispr-pacman.stanford.edu/) to disseminate Cas13d crRNAs that target a broad spectrum of RNA viruses. We experimentally tested a group of predicted crRNAs targeting SARS-CoV-2 genomes and found a high correlation between predicted and validated efficiency. We found that five highly efficient crRNAs can target all of the known SARS-CoV-2 strains, including new variants. This work provides a comprehensive analysis and useful resource for using PAC-MAN to target a broad spectrum of pathogenic RNA viruses and can facilitate the development of CRISPR-based antiviral technology.

RESULTS

An integrated pipeline for Cas13 crRNA analysis for virus-targeting coverage, efficiency, and specificity

We retrieved RNA virus genomes from public databases, including 16 RNA virus families from the ViPR, HIV from NCBI,[12] and IAV from the Influenza Research Database (IRD)[13] (Table S1). Our pipeline analyzed conserved genome sequences within a designated group of viruses, which generated the primary regions for crRNA targeting (Figure 1A). We generated all possible crRNA candidates with perfect matches to the conserved sequence. The pipeline eliminated crRNAs with putative off-target binding in the human transcriptome ($\leq$2 mismatches, a threshold that was previously defined to distinguish specific versus non-specific crRNAs[14]). We incorporated a recently reported algorithm to predict crRNA efficiency (range 0–1) and also computed for each crRNA the percentage of viral strains in the group that it targets. We used our pipeline to analyze two types of crRNAs with different features. The first type is species-specific crRNAs, which are comprehensive sets of crRNAs that can target conserved regions in closely related branches of viruses with high coverage, specificity, and predicted efficiency. The second type is family-covering crRNAs, which are minimal pools of crRNAs ("minipools") that collectively target every virus in a given family.

Targeting pandemic/epidemic-causing pathogenic RNA virus species using PAC-MAN

We identified species-specific crRNA sets targeting each pandemic/epidemic-causing pathogenic RNA virus species per the WHO; these viruses include SARS, SARS-CoV-2, MERS, Ebola virus, Marburg virus, Zika virus, Chikungunya virus, and Nipah virus. For most pathogenic virus species, we were able to obtain a collection of crRNAs with predicted high specificity ($\geq$3 mismatches in the human transcriptome), high efficiency (score $\geq$ 0.5), and high coverage (targets >90% of viruses in the group with zero mismatches) (Figure 1B). One exception was Nipah virus, for which we found that no crRNA candidate was able to cover 90% of sequenced strains. Nevertheless, lowering the coverage requirement to 80% virus strain coverage produced a set of crRNAs that can target the Nipah virus.

Analysis of PAC-MAN for targeting a broad spectrum of RNA viruses

We next identified crRNAs that can be used to target a broad spectrum of RNA virus families. We analyzed 10 RNA virus families (calicividirae, coronaviridae, filoviridae, hepeviridae, paramyxoviridae, phenuiviridae, picornaviridae, pneumoviridae, rhabdoviridae, and togaviridae) from the ViPR database that infect various human organs and systems, including 6 positive-sense single-stranded RNA (ssRNA) virus families, 4 negative-sense ssRNA virus families, as well as HIV and IAV species (Figure 1C). For each family or HIV/IAV species, we used an approximation algorithm to obtain a minipool of crRNAs that can collectively target every strain in the family.

Interestingly, we observed that all human-infectious sequences for each of the 10 RNA virus families and HIV can be comprehensively targeted by a small minipool of crRNAs (3–23 crRNAs). One exception is IAV, which requires 78 crRNAs for comprehensive coverage, likely due to its high diversity and its segmented genome, which is split into 8 segments[15] (Figure 1D). Since many families contain rare strains with highly variant genomes, if we aim to target at least 90% of viral strains, then the human-infectious members of each family can be targeted by a very small number (1–6) of crRNAs (Figure 1E).

Crucially, we found that a minipool of 14 crRNAs is able to target >90% of human-infectious viruses in the 10 RNA virus families (Figures 1F and S1A). A complete minipool of 90 crRNAs can target all human-infectious strains (24,096) in the 10 families with zero mismatches. We observed that the 14 minipool crRNAs target notable pathogenic viral species with zero mismatches (Figure 1G). This suggests that Cas13-mediated PAC-MAN may offer a potential broad-spectrum antiviral (BSA) strategy for broadly targeting human infectious RNA viruses.

We also analyzed crRNAs that can target animal viruses. For this purpose, we categorized viruses according to their host, including common domestic livestock (cattle, sheep, pig, cat, and dog) that have close interactions with humans. For each category of virus, we observed that a small minipool of crRNAs was able to target the majority of viruses (Figures 1H and S1B). This analysis suggests that beyond human-infectious viruses, PAC-MAN may be used as a BSA strategy in animals, a field that is underdeveloped in the biotechnology sector.

Determinants required of crRNAs targeting a broad spectrum of RNA virus families

We further analyzed whether families with more virus strains required more minipool crRNAs to achieve comprehensive targeting. For the 10 RNA virus families analyzed, we observed a linear relationship between the number of human-infectious strains and the number of crRNAs in the minipool targeting these strains ($R = 0.70$, $p = 0.023$; Figure 2A). When we examined all of the strains in each family and the corresponding minipools targeting these strains, we observed a similar linear relationship

(F) A cumulative curve showing the predicted minimum number of crRNAs to target all human-infectious strains in 10 RNA virus families in (C).
(G) Coverage of pathogenic RNA viruses by the first 14 crRNAs in the minipool from (F).
(H) A cumulative curve showing the predicted minimum number of crRNAs to target livestock-infectious strains in 10 RNA virus families in (C). Bovine, ovine, swine, feline, and canine viruses are included in the analysis.
See also Figure S1 and Table S1.

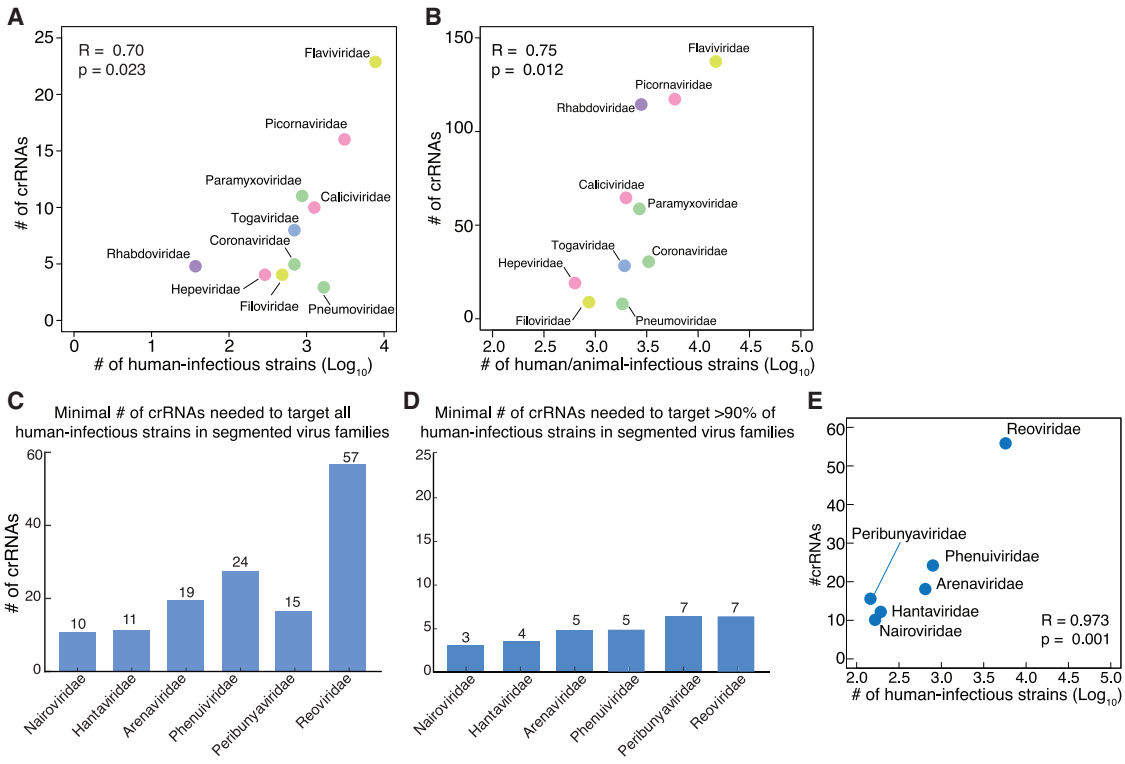

Figure 2. Determinants of required crRNAs targeting broad-spectrum RNA virus families

(A) Correlation between the number of human-infectious strains in each RNA virus family and the number of crRNAs needed for targeting those strains.

(B) Correlation between the number of strains in each RNA virus family and the number of crRNAs needed for targeting all of the strains in that family.

(C) The number of crRNAs needed to target all of the sequenced human-infectious strains in each of 6 RNA virus families with segmented genomes.

(D) The number of crRNAs needed to target 90% of sequenced human-infectious strains in each of 6 RNA virus families with segmented genomes.

(E) Correlation between the number of strains in the RNA virus family and the number of crRNAs needed for targeting all human-infectious viruses in 6 segmented RNA virus families.

(R = 0.75. p = 0.012; Figure 2B). This suggests that, as expected, the number of minipool crRNAs required to comprehensively target all of the strains in an RNA virus family is strongly influenced by the number of strains in that family.

The observation that IAV requires more crRNAs for coverage compared to the other 10 families and HIV inspired us to analyze more RNA virus families with segmented genomes. To do this, we included 6 segmented RNA virus families, including 5 negative-sense ssRNA virus families and 1 double-stranded RNA (dsRNA) virus family. Interestingly, we observed that segmented RNA virus families generally require larger minipools to comprehensively target all of the human-infectious strains in that family (10-57 crRNAs for full coverage and 3-7 crRNAs for 90% coverage; Figures 2C and 2D). This is likely due to the reassortment process, a shared feature in segmented RNA viruses that have the capacity to exchange genome segments during co-infection.[16] Reassortment may greatly increase the diversity of segmented viral genome sequences, making it more challenging to define very few crRNAs to broadly cover strains. Despite the nature of these segmented genomes, we still observed that the number of required minipool crRNAs for comprehensive coverage of human-infectious strains is strongly correlated with the number of human-infectious strains in that family (R = 0.973 , p = 0.001 ; Figure 2E). Overall, our data suggest that PAC-MAN is most effective against non-segmented RNA virus families for broad-spectrum targeting.

An online resource to use CRISPR-Cas13d for BSA targeting

We built an online resource (http://crispr-pacman.stanford.edu) to facilitate the dissemination of analyzed Cas13d crRNAs for 16 RNA virus families, as well as for HIV, IAV, and influenza B virus (IBV). For species-specific crRNAs in each family, we defined a library of crRNAs with predicted high specificity ($\geq$3 mismatches in the human transcriptome and no target in other species in the same family) and high efficiency (score $\geq$0.5). We provided an interactive tool to facilitate the choice of crRNAs targeting specific genes on a virus. We also implemented a graphical user interface (GUI) for SARS-CoV-2, which integrates with the University of California, Santa Cruz (UCSC) Genome Browser[17] and creates a visualization for the mapping of crRNAs to sequence position along the annotated viral genome. An example is provided to visualize where predicted crRNAs target the SARS-CoV-2 genome (Figures 3A–3C). For family-covering crRNAs, we included a phylogenetic tree generated using the Interactive Tree Of Life (iTOL) tool to visualize the evolutionary

CellPress
OPEN ACCESS

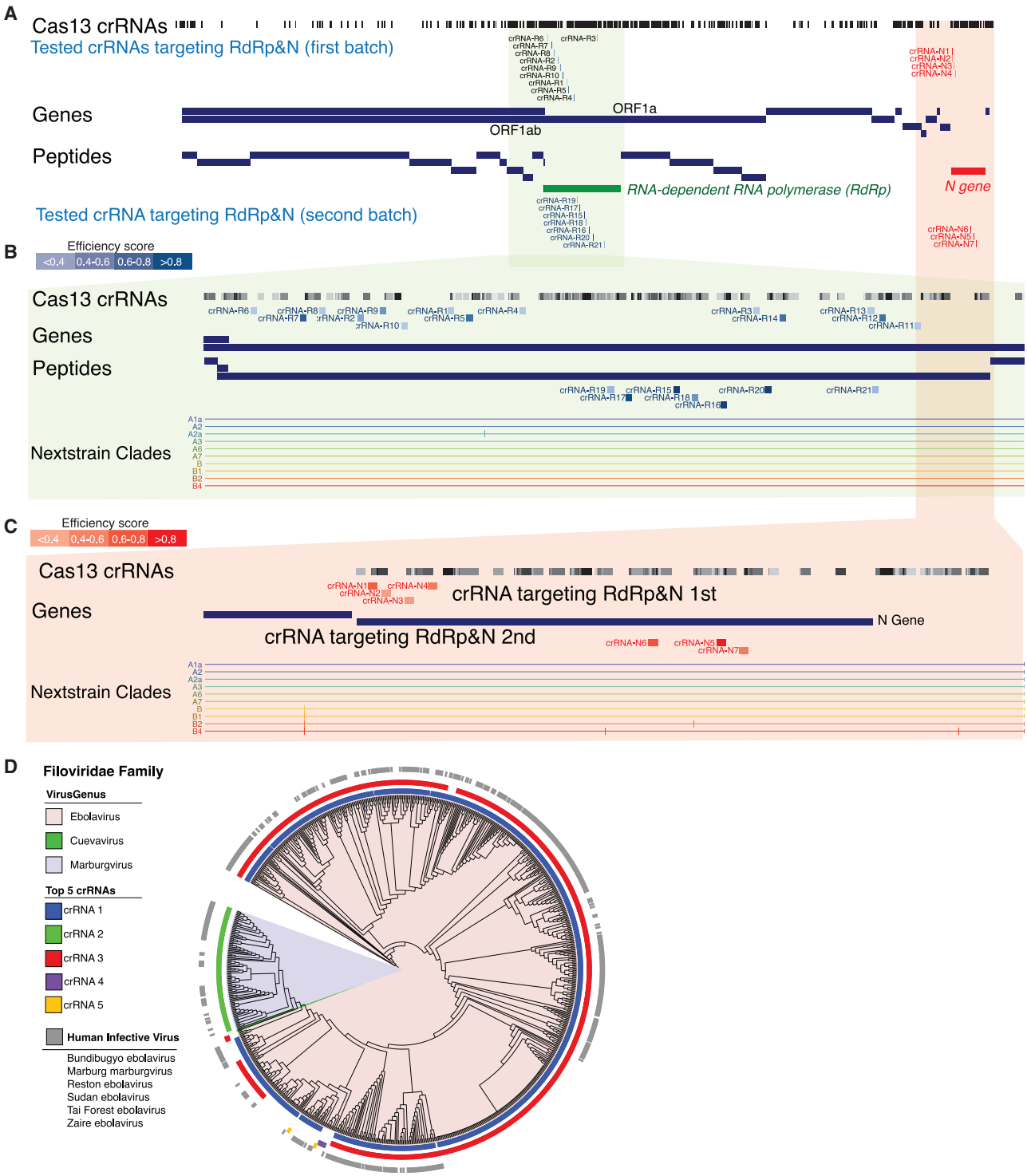

Figure 3. CRIPSR-PACMAN as an online resource of using CRISPR-Cas13d for broad-spectrum antiviral targeting

(A–C) An exemplar diagram showing the crRNAs designed to target SARS-CoV-2 and its alignment to the genes of SARS-CoV-2. These crRNAs are used for testing in Figure 4. The intensity of colors for each crRNA represents its predicted crRNA score.

(D) An exemplar diagram showing the analysis of family-covering crRNAs targeting the Filoviridae family, including Ebola virus.

See also Table S2.

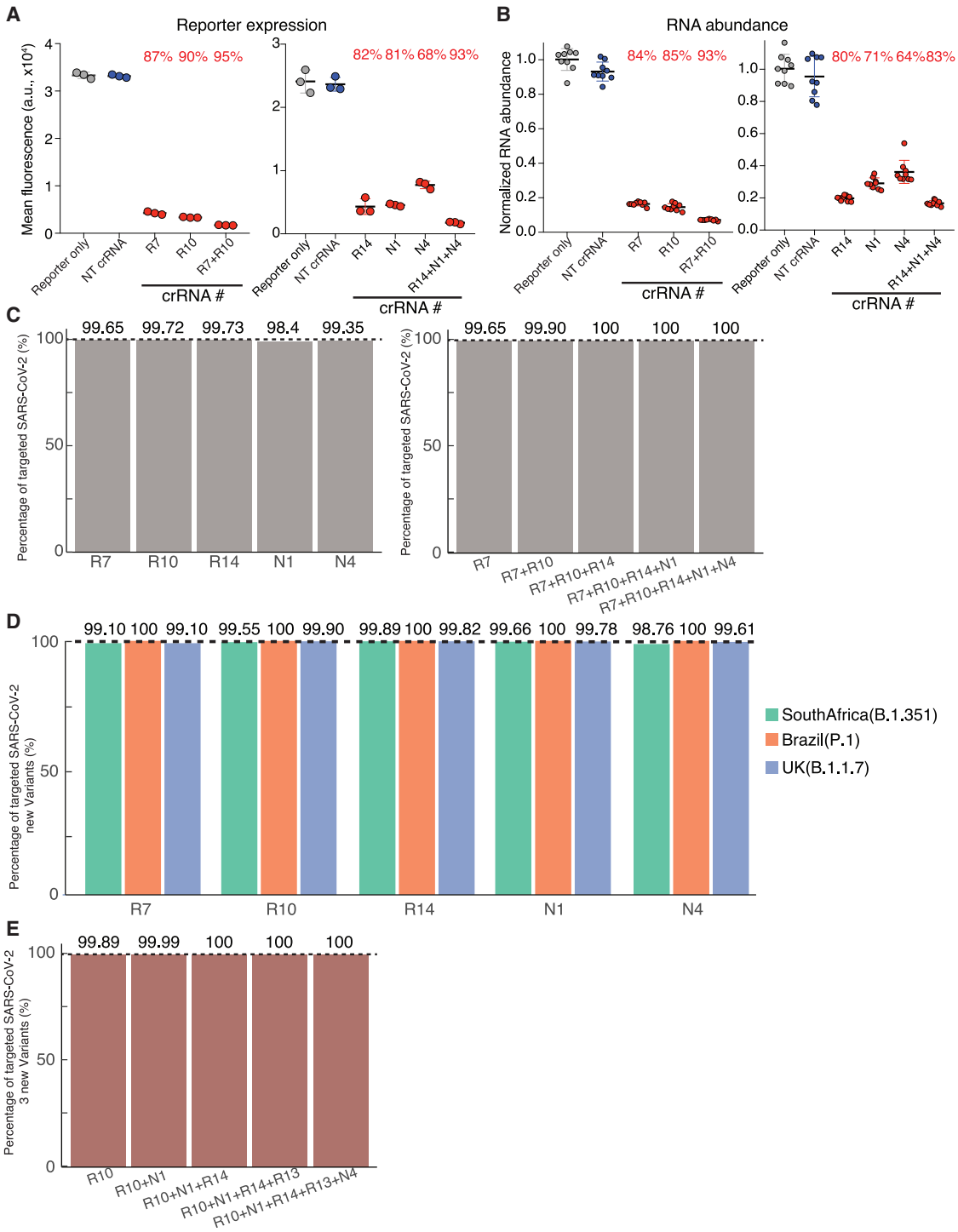

Figure 4. Optimized crRNAs targeting SARS-CoV-2 sequences using CRISPR-PAC-MAN

(A and B) Repression effects of the optimized minipool of crRNAs (crRNA-MP5) on SARS-CoV-2 GFP reporter (A) and RNA abundance (B).

(A) GFP expression as measured by flow cytometry. p values for each group are included in Table S3. Lines indicate means; error bars indicate SDs (n = 3 independent biological replicates).

(B) mRNA abundance as measured by quantitative real-time PCR. Relative RNA abundance is calculated by normalizing to the reporter-only sample. p values for each group are included in Table S3. Lines indicate means; error bars indicate SDs. The data represent 3 independent biological experiments performed in technical replicates (n = 9).

(legend continued on next page)

relationship of the strains targeted by each crRNA.[18] We annotated each viral strain in the phylogenetic tree with the genus that the strain belongs to, whether the strain is a human host, and which (if any) of the first 5 crRNAs in the family-covering minipool targets the strain. We provided an example of this phylogenetic tree visualizing family-covering crRNAs for the Filoviridae family, a viral family that includes the pandemic Ebola virus (Figure 3D). We created a video to provide an overview of this online resource (Video S1).

Validation of predicted crRNAs for targeting SARS-CoV-2 sequences

We next experimentally validated whether the predicted species-specific crRNAs enabled effective Cas13d-mediated inhibition of the SARS-CoV-2 sequence. We used our recently reported SARS-CoV-2 reporters, F1 and F2, which encode a GFP gene fused to SARS-CoV-2 sequences encoding RNA-dependent RNA polymerase (RdRP), which maintains virus proliferation, or nucleocapsid (N), which controls viral packaging[19] (Figure S2A). The Cas13d and crRNA were expressed using 2 plasmids, as reported before (Figure S2B). To measure the inhibitory effects of crRNAs, we co-transfected individual crRNA plasmids and SARS-CoV-2 reporter plasmids into A549 lung epithelial cells that expressed Cas13d, and quantified GFP expression using flow cytometry and target RNA abundance using quantitative PCR (qPCR) 48 h post transfection (Figure S2C).

We designed a list of crRNAs targeting RdRP or N without efficiency prediction (Figures 3B and 3C; Table S2). We observed varying repressive effects on the SARS-CoV-2 reporters of individual crRNAs using flow cytometry (Figure S3A; Table S3). Interestingly, there was a statistically significant high correlation between the percentage of GFP repression and the predicted efficiency scores, which were obtained by using a recently reported algorithm[14] ($R = 0.834$, $p = 1.667 \times 10^{-5}$; Figure S3B). These results were consistent with the repressive effects on RNA abundance as measured by qPCR ($R = 0.812$, $p = 4.302 \times 10^{-5}$; Figures S3C and S3D; Table S4). These data together suggest that the reported algorithm was able to faithfully predict efficient crRNAs for viral genome targeting, despite it being developed based on data from crRNAs targeting human transcripts.

To further validate the performance of the predicted crRNAs, we tested more predicted crRNAs targeting the SARS-CoV-2 sequence with varying efficiency scores (Figures 3B and 3C). Again, we observed a strong correlation between the predicted efficiency and the measured reporter repression ($R = 0.875$, $p = 0.0009$; Figures S3E and S3F). We noticed a binary trend: most crRNAs with an efficiency score >0.5 showed efficient repression, whereas crRNAs with an efficiency score <0.5 showed almost no repression. This justified our choice of 0.5 as the threshold to determine efficient crRNAs. These independent experiments confirmed the efficacy of the predicted crRNAs using the algorithm, which also suggests that our computational pipeline can be used to suggest crRNAs that will efficiently inhibit other RNA virus sequences.

Optimized crRNAs targeting SARS-CoV-2 sequences using CRISPR-PAC-MAN

Finally, we defined a minipool of 5 highly efficient crRNAs (crRNA-MP5) targeting sequenced SARS-CoV-2 genomes. Using SARS-CoV-2 reporters, we confirmed that individual crRNAs could repress GFP up to 90% (Figure 4A), with an 85% repression of RNA abundance (Figure 4B). Pooling these crRNAs further enhanced repression up to 95% for GFP expression and 93% for RNA abundance. We further retrieved sequences of 351,670 SARS-CoV-2 isolates from the Global Initiative on Sharing All Influenza Data (GISAID)[20] database (as of January 16, 2021). Each crRNA in crRNA-MP5 was able to target almost 99% of SARS-CoV-2 isolates, and the crRNA-MP5 together can target all of the known SARS-CoV-2 strains regardless of the variations in different SARS-CoV-2 clades as identified in Nextstrain[21] (Figure 4C). Three new SARS-CoV-2 variants, including the UK variant (B.1.1.7),[22] the South Africa variant (B.1.351),[23] and the Brazil variant (P.1)[24] have emerged since the autumn of 2020. Although multiple mutations have been detected in these new SARS-CoV-2 variants, most reside in the Spike gene and fewer are in the regions targeted by our chosen crRNAs (e.g., RdRP, N). Each crRNA in crRNA-MP5 could still target ~99% of isolates from each variant (Figure 4D), which were downloaded from GISAID on February 3, 2021. Of note, the coverage of each crRNA-MP5 for the Brazil strain was 100%. The crRNA-MP5 together can target all of the sequenced strains in these 3 variants (Figure 4E). In summary, the optimized minipool of crRNA-MP5 provides a useful resource to be tested against live SARS-CoV-2 virus *in vitro* and *in vivo* in the future.

DISCUSSION

The rapid development of CRISPR-Cas13-based antivirals has raised the question of whether the system can be effectively used to broadly target many families of RNA viruses. Here, we perform a comprehensive *in silico* analysis using CRISPR-Cas13 to target notable pathogenic viral species and 16 families of human- or animal-infectious RNA viruses in the ViPR database. Our integrated crRNA analysis pipeline incorporates existing algorithms and computes the coverage, efficiency, and specificity of crRNAs for RNA virus targeting. We observed that 10 families of human-infectious viruses can be flexibly targeted by a minipool of 14 crRNAs with >90% coverage. We determined that strain count, diversity, and genome segmentation are potential determinant factors for the number of crRNAs required to comprehensively target a family of viruses. We also observed that, similar to human-infectious viruses, PAC-MAN may also provide a BSA strategy for viruses that infect domestic livestock, thus expanding its potential applications.

(C) Bar graphs showing the percentage of genomes of SARS-CoV-2 isolates targeted by individual or multiple crRNAs in the optimized crRNA minipool.
(D and E) Bar graphs showing the percentage of genomes of 3 new SARS-CoV-2 variants targeted by individual (D) or multiple crRNAs (E) in the optimized crRNA minipool.
See also Figures S2 and S3 and Tables S3 and S4.

Importantly, the crRNAs designed here can target all sequenced new SARS-CoV-2 strains to date. Given the rapid development of CRISPR-Cas13 as antivirals against SARS-CoV-2 and other RNA viruses,[25] this work provides a resource to the community for using CRISPR-Cas13 PAC-MAN for broad-spectrum targeting with potential use in the development of antivirals.

One major advantage of the PAC-MAN system is its potential as a BSA due to easy multiplexed targeting ability of the CRISPR-Cas13 system. The Cas13 system can use a crRNA minipool or process multiple crRNAs from a crRNA array to target different genes or strains simultaneously. One study demonstrated that 4 crRNAs can be simultaneously delivered in a simple arrayed vector and efficiently knock down 4 target transcripts.[26] Using more crRNAs to target many viruses simultaneously will likely require several technical issues to be addressed, including the efficient expression of long crRNA arrays and efficient Cas13d processing of the crRNA arrays. For example, higher expression of the Cas13d protein may help each crRNA pair with Cas13d, thus mitigating the dilution of crRNAs and increasing the knockdown efficiency.[2]

We further provided an online resource to disseminate specific, efficient, broad-coverage crRNAs targeting RNA viruses. We built a website (http://crispr-pacman.stanford.edu/) with a useful graphical user interface and interactive functionality to facilitate easy access to CRISPR PAC-MAN crRNAs for the broad research community. We experimentally tested different sets of predicted crRNAs targeting the SARS-CoV-2 genomes and found a strong correlation between predicted and validated efficiency. The target site nucleotide context and the secondary structure of mRNA are the major factors determining crRNA targeting efficiency.[14] The mRNAs produced from the SARS-CoV-2 reporter plasmid and RNAs from live SARS-CoV-2 virus have the same sequence and likely similar local secondary structure. Although additional experiments examining the inhibitory efficiency of crRNAs *in vivo* with live viruses are required to confirm this strong correlation, the observed high efficiency of these guides in our study provides a proof-of-concept of the utility of the designed crRNAs against diverse RNA viruses. In summary, this work provides a bioinformatic tool and an online resource for using CRISPR-Cas13-mediated PAC-MAN for BSA targeting with potential future applications in the development of antiviral therapies.

Limitations of study

Although CRISPR-PAC-MAN provides a potential antiviral strategy to combat RNA viruses, there are several challenges that need to be addressed before it enters practical clinical use. For BSA targeting, it remains unknown whether the current CRISPR-Cas13d system can effectively handle the scale of 14 crRNAs simultaneously for the efficient knockdown of each target. Further technical investigation and optimization are needed. Furthermore, delivery is key to successful applications of PAC-MAN in the human body. Conceptually, a sufficiently high delivery threshold is required for efficient use of PAC-MAN against viral infection. Toward this goal, various strategies are being investigated. These strategies include the delivery of mRNA encoding Cas13d and crRNAs using liposomes or lipid nanoparticles[27–31] or delivery of the ribonucleoprotein (RNP) complex containing the Cas13d protein and crRNA to airway epithelia.[32–34] Cas13d and crRNAs can also be delivered using adenovirus or adeno-associated virus (AAV).[35–37] Such delivery modalities could be administered to populations via a nebulizer system or nasal spray, which may present a convenient and cost-effective form of antivirals in pandemics. In the present study, we used A549 human lung epithelial carcinoma cells to validate the targeting efficiency of SARS-CoV-2 sequences by predicted crRNAs (Figure S3). A549 cells have been engineered to stably express Cas13d, and crRNAs were introduced via lentiviral transduction to quantify knockdown efficiency. In future studies, the use of primary cells or an air-liquid interface (ALI) culture system[38] will better mimic the tracheobronchial epithelium of the human respiratory tract to study the inhibition in live SARS-CoV-2 virus infection.

STAR★METHODS

Detailed methods are provided in the online version of this paper and include the following:

- KEY RESOURCES TABLE
- RESOURCE AVAILABILITY
  - Lead contact
  - Materials availability
  - Data and code availability
- EXPERIMENTAL MODEL AND SUBJECT DETAILS
  - Cell culture
- METHOD DETAILS
  - A general pipeline for crRNA analysis
  - Format of dataset in CRISPR-PAC-MAN server
  - SARS-CoV-2 targeting in CRISPR-PACMAN
  - Design and cloning of RdRP- and N-targeting crRNAs
  - Design and cloning of SARS-CoV-2 reporters
  - Lentiviral packaging and cell line generation
  - SARS-CoV-2 reporter challenge experiments
  - Quantitative RT-PCR (qRT-PCR)
- QUANTIFICATION AND STATISTICAL ANALYSIS
  - Flow cytometry
  - Quantitative RT-PCR (qRT-PCR)

SUPPLEMENTAL INFORMATION

Supplemental information can be found online at https://doi.org/10.1016/j.xcrm.2021.100245.

ACKNOWLEDGMENTS

The authors thank all of the members from the Stanley Qi lab for useful comments and help on experiments and manuscript preparation. The authors thank David Lewis for helpful insights. The authors thank the researchers who generated and contributed the SARS-CoV-2 sequence data to GISAID (https://www.gisaid.org/). The project is supported by a contract grant from the Defense Advanced Research Projects Agency (DARPA; grant no. HR001119C0060), a COVID-19 Research and Assistance Fund from the School of Engineering at Stanford University, and gift funds from the Li Ka Shing Foundation and the Lucile Packard Foundation for Children's Health.

AUTHOR CONTRIBUTIONS

X.L., Y.L., A.C., and L.S.Q. conceived the study. X.L., A.C., and M.L.R. designed and developed the platform. Y.L. designed and performed the experiments. T.P. prepared the tutorial video. X.L., A.C., Y.L., and L.S.Q. wrote the manuscript. All of the authors read and commented on the manuscript.

DECLARATION OF INTERESTS

Provisional patents have been filed via Stanford University related to the work.

Received: September 9, 2020
Revised: February 20, 2021
Accepted: March 17, 2021
Published: March 23, 2021

REFERENCES

1. De Clercq, E., and Li, G. (2016). Approved Antiviral Drugs over the Past 50 Years. Clin. Microbiol. Rev. *29*, 695–747.
2. Abbott, T.R., Dhamdhere, G., Liu, Y., Lin, X., Goudy, L., Zeng, L., Chemparathy, A., Chmura, S., Heaton, N.S., Debs, R., et al. (2020). Development of CRISPR as an Antiviral Strategy to Combat SARS-CoV-2 and Influenza. Cell *181*, 865–876.e12.
3. Singsuksawat, E., Onnome, S., Posiri, P., Suphatrakul, A., Srisuk, N., Nantachokchawapan, R., Praneechit, H., Sae-kow, C., Chidpratum, P., Hongeng, S., et al. (2020). Potent Programmable Antiviral Against Dengue Virus in Primary Human Cells by Cas13b Rnp with Short Spacer and Delivery by Virus-Like Particle. bioRxiv. https://doi.org/10.1101/2020.05.17.100388.
4. Li, H., Wang, S., Dong, X., Li, Q., Li, M., Li, J., Guo, Y., Jin, X., Zhou, Y., Song, H., and Kou, Z. (2020). CRISPR-Cas13a Cleavage of Dengue Virus NS3 Gene Efficiently Inhibits Viral Replication. Mol. Ther. Nucleic Acids *19*, 1460–1469.
5. Freije, C.A., Myhrvold, C., Boehm, C.K., Lin, A.E., Welch, N.L., Carter, A., Metsky, H.C., Luo, C.Y., Abudayyeh, O.O., Gootenberg, J.S., et al. (2019). Programmable Inhibition and Detection of RNA Viruses Using Cas13. Mol. Cell *76*, 826–837.e11.
6. Yin, L., Zhao, F., Sun, H., Wang, Z., Huang, Y., Zhu, W., Xu, F., Mei, S., Liu, X., Zhang, D., et al. (2020). CRISPR-Cas13a Inhibits HIV-1 Infection. Mol. Ther. Nucleic Acids *21*, 147–155.
7. Mahas, A., Aman, R., and Mahfouz, M. (2019). CRISPR-Cas13d mediates robust RNA virus interference in plants. Genome Biol. *20*, 263.
8. Aman, R., Mahas, A., Butt, H., Aljedaani, F., and Mahfouz, M. (2018). Engineering RNA Virus Interference via the CRISPR/Cas13 Machinery in Arabidopsis. Viruses *10*, 732.
9. Bawage, S.S., Tiwari, P.M., and Santangelo, P.J. (2018). Synthetic mRNA expressed Cas13a mitigates RNA virus infections. bioRxiv. https://doi.org/10.1101/370460.
10. Gootenberg, J.S., Abudayyeh, O.O., Kellner, M.J., Joung, J., Collins, J.J., and Zhang, F. (2018). Multiplexed and portable nucleic acid detection platform with Cas13, Cas12a, and Csm6. Science *360*, 439–444.
11. Pickett, B.E., Sadat, E.L., Zhang, Y., Noronha, J.M., Squires, R.B., Hunt, V., Liu, M., Kumar, S., Zaremba, S., Gu, Z., et al. (2012). ViPR: an open bioinformatics database and analysis resource for virology research. Nucleic Acids Res. *40*, D593–D598.
12. Sayers, E.W., Barrett, T., Benson, D.A., Bolton, E., Bryant, S.H., Canese, K., Chetvernin, V., Church, D.M., DiCuccio, M., Federhen, S., et al. (2011). Database resources of the National Center for Biotechnology Information. Nucleic Acids Res. *39*, D38–D51.
13. Squires, R.B., Noronha, J., Hunt, V., García-Sastre, A., Macken, C., Baumgarth, N., Suarez, D., Pickett, B.E., Zhang, Y., Larsen, C.N., et al. (2012). Influenza research database: an integrated bioinformatics resource for influenza research and surveillance. Influenza Other Respir. Viruses *6*, 404–416.
14. Wessels, H.-H., Méndez-Mancilla, A., Guo, X., Legut, M., Daniloski, Z., and Sanjana, N.E. (2020). Massively parallel Cas13 screens reveal principles for guide RNA design. Nat. Biotechnol. *38*, 722–727.
15. McGeoch, D., Fellner, P., and Newton, C. (1976). Influenza virus genome consists of eight distinct RNA species. Proc. Natl. Acad. Sci. USA *73*, 3045–3049.
16. McDonald, S.M., Nelson, M.I., Turner, P.E., and Patton, J.T. (2016). Reassortment in segmented RNA viruses: mechanisms and outcomes. Nat. Rev. Microbiol. *14*, 448–460.
17. Fernandes, J.D., Hinrichs, A.S., Clawson, H., Navarro Gonzalez, J., Lee, B.T., Nassar, L.R., Raney, B.J., Rosenbloom, K.R., Nerli, S., Rao, A.A., et al. (2020). The UCSC SARS-CoV-2 Genome Browser. Nat. Genet. *52*, 991–998.
18. Letunic, I., and Bork, P. (2019). Interactive Tree Of Life (iTOL) v4: recent updates and new developments. Nucleic Acids Res. *47* (*W1*), W256–W259.
19. Wu, F., Zhao, S., Yu, B., Chen, Y.M., Wang, W., Song, Z.G., Hu, Y., Tao, Z.W., Tian, J.H., Pei, Y.Y., et al. (2020). A new coronavirus associated with human respiratory disease in China. Nature *579*, 265–269.
20. Shu, Y., and McCauley, J. (2017). GISAID: global initiative on sharing all influenza data - from vision to reality. Euro Surveill. *22*, 30494.
21. Hadfield, J., Megill, C., Bell, S.M., Huddleston, J., Potter, B., Callender, C., Sagulenko, P., Bedford, T., and Neher, R.A. (2018). Nextstrain: real-time tracking of pathogen evolution. Bioinformatics *34*, 4121–4123.
22. Horby, P., Huntley, C., Davies, N., Edmunds, J., Ferguson, N., Medley, G., and Semple, C. (2021). NERVTAG note on B. 1.1. 7 severity. https://www.gov.uk/government/publications/nervtag-paper-on-covid-19-variant-of-concern-b117.
23. Rambaut, A., Holmes, E.C., O'Toole, Á., Hill, V., McCrone, J.T., Ruis, C., du Plessis, L., and Pybus, O.G. (2020). A dynamic nomenclature proposal for SARS-CoV-2 lineages to assist genomic epidemiology. Nat. Microbiol. *5*, 1403–1407.
24. Faria, N.R., Claro, I.M., Candido, D., Moyses Franco, L.A., Andrade, P.S., Coletti, T.M., Silva, C.A.M., Sales, F.C., Manuli, E.R., Aguiar, R.S., et al.; CADDE Genomic Network (2021). Genomic characterisation of an emergent SARS-CoV-2 lineage in Manaus: preliminary findings. https://virological.org/t/genomic-characterisation-of-an-emergent-sars-cov-2-lineage-in-manaus-preliminary-findings/586.
25. Blanchard, E.L., Vanover, D., Bawage, S.S., Tiwari, P.M., Rotolo, L., Beyersdorf, J., Peck, H.E., Bruno, N.C., Hincapie, R., Michel, F., et al. (2021). Treatment of influenza and SARS-CoV-2 infections via mRNA-encoded Cas13a in rodents. Nat. Biotechnol. Published online February 3, 2021. https://doi.org/10.1038/s41587-021-00822-w.
26. Konermann, S., Lotfy, P., Brideau, N.J., Oki, J., Shokhirev, M.N., and Hsu, P.D. (2018). Transcriptome Engineering with RNA-Targeting Type VI-D CRISPR Effectors. Cell *173*, 665–676.e14.
27. Huang, C.-Y., Uno, T., Murphy, J.E., Lee, S., Hamer, J.D., Escobedo, J.A., Cohen, F.E., Radhakrishnan, R., Dwarki, V., and Zuckermann, R.N. (1998). Lipitoids–novel cationic lipids for cellular delivery of plasmid DNA in vitro. Chem. Biol. *5*, 345–354.
28. Hendel, A., Bak, R.O., Clark, J.T., Kennedy, A.B., Ryan, D.E., Roy, S., Steinfeld, I., Lunstad, B.D., Kaiser, R.J., Wilkens, A.B., et al. (2015). Chemically modified guide RNAs enhance CRISPR-Cas genome editing in human primary cells. Nat. Biotechnol. *33*, 985–989.
29. McKinlay, C.J., Vargas, J.R., Blake, T.R., Hardy, J.W., Kanada, M., Contag, C.H., Wender, P.A., and Waymouth, R.M. (2017). Charge-altering releasable transporters (CARTs) for the delivery and release of mRNA in living animals. Proc. Natl. Acad. Sci. USA *114*, E448–E456.
30. Sago, C.D., Lokugamage, M.P., Paunovska, K., Vanover, D.A., Monaco, C.M., Shah, N.N., Gamboa Castro, M., Anderson, S.E., Rudoltz, T.G., Lando, G.N., et al. (2018). High-throughput in vivo screen of functional

mRNA delivery identifies nanoparticles for endothelial cell gene editing. Proc. Natl. Acad. Sci. USA *115*, E9944–E9952.

31. Handumrongkul, C., Ye, A.L., Chmura, S.A., Soroceanu, L., Mack, M., Ice, R.J., Thistle, R., Myers, M., Ursu, S.J., Liu, Y., et al. (2019). Durable multi-transgene expression in vivo using systemic, nonviral DNA delivery. Sci. Adv. *5*, eaax0217.
32. Amirkhanov, R.N., and Stepanov, G.A. (2019). Systems of delivery of CRISPR/Cas9 ribonucleoprotein complexes for genome editing. Russ. J. Bioorganic Chem. *45*, 431–437.
33. Krishnamurthy, S., Wohlford-Lenane, C., Kandimalla, S., Sartre, G., Meyerholz, D.K., Théberge, V., Hallée, S., Duperré, A.M., Del'Guidice, T., Lepetit-Stoffaes, J.P., et al. (2019). Engineered amphiphilic peptides enable delivery of proteins and CRISPR-associated nucleases to airway epithelia. Nat. Commun. *10*, 4906.
34. Xu, C.-F., Chen, G.-J., Luo, Y.-L., Zhang, Y., Zhao, G., Lu, Z.D., Czarna, A., Gu, Z., and Wang, J. (2021). Rational designs of in vivo CRISPR-Cas delivery systems. Adv. Drug Deliv. Rev. *168*, 3–29.
35. Halbert, C.L., Allen, J.M., and Miller, A.D. (2001). Adeno-associated virus type 6 (AAV6) vectors mediate efficient transduction of airway epithelial cells in mouse lungs compared to that of AAV2 vectors. J. Virol. *75*, 6615–6624.
36. Santry, L.A., Ingrao, J.C., Yu, D.L., de Jong, J.G., van Lieshout, L.P., Wood, G.A., and Wootton, S.K. (2017). AAV vector distribution in the mouse respiratory tract following four different methods of administration. BMC Biotechnol. *17*, 43.
37. van Lieshout, L.P., Domm, J.M., and Wootton, S.K. (2019). AAV-Mediated Gene Delivery to the Lung. Methods Mol. Biol. *1950*, 361–372.
38. Sungnak, W., Huang, N., Bécavin, C., Berg, M., Queen, R., Litvinukova, M., Talavera-López, C., Maatz, H., Reichart, D., Sampaziotis, F., et al.; HCA Lung Biological Network (2020). SARS-CoV-2 entry factors are highly expressed in nasal epithelial cells together with innate immune genes. Nat. Med. *26*, 681–687.
39. Nakamura, T., Yamada, K.D., Tomii, K., and Katoh, K. (2018). Parallelization of MAFFT for large-scale multiple sequence alignments. Bioinformatics *34*, 2490–2492.
40. Langmead, B., Trapnell, C., Pop, M., and Salzberg, S.L. (2009). Ultrafast and memory-efficient alignment of short DNA sequences to the human genome. Genome Biol. *10*, R25.
41. Langmead, B., and Salzberg, S.L. (2012). Fast gapped-read alignment with Bowtie 2. Nat. Methods *9*, 357–359.

STAR★METHODS

KEY RESOURCES TABLE

REAGENT or RESOURCE	SOURCE	IDENTIFIER
Bacterial and virus strains		
Stellar chemically competent cells	TaKaRa	Cat# 636766
Chemicals, peptides, and recombinant proteins		
Puromycin	Gold Biotech	Cat# P-600-1
Fetal Bovine Serum (FBS)	Clontech	Cat# 631367
Trypsin-EDTA solution	Sigma	Cat# T4049-100ML
DMEM	ThermoFisher Scientific	Cat# 10569-044
Mirus TransIT-LT1	Mirus Bio	Cat# MIR 2306
Experimental models: Cell lines		
HEK293T	ATCC	Cat# CRL-3216; RRID: CVCL_0063
A549	ATCC	Cat# CCL-185; RRID: CVCL_0023
A549 + Cas13d (pSLQ5428)	Abbott et al.[2]	N/A
Oligonucleotides		
Primer used in qPCR: SARS-COV-F1_F: 5′-AACGGGTTTGCGGTGTAAGT-3′	Abbott et al.[2]	N/A
Primer used in qPCR: SARS-COV-F1_R: 5′-AA TTTAGCAAAACCAGCTACTTTATCATTGTAG-3′	Abbott et al.[2]	N/A
Primer used in qPCR: SARS-COV-F2_F: 5′-CAGGTGGAACCTCATCAGGAG-3′	Abbott et al.[2]	N/A
Primer used in qPCR: SARS-COV-F2_R: 5′-GTT ACCATCAGTAGATAAAAGTGCATTAACATTG-3′	Abbott et al.[2]	N/A
Primer used in qPCR: GAPDH_F: 5′-TGCACCACCAACTGCTTAGC-3′	Abbott et al.[2]	N/A
Primer used in qPCR: GAPDH_R: 5′-GGCATGGACTGTGGTCATGAG-3′	Abbott et al.[2]	N/A
Recombinant DNA		
pHR-PGK-sfGFP-SARS-COV-F1	Abbott et al.[2]	N/A
pHR-PGK-sfGFP-SARS-COV-F2	Abbott et al.[2]	N/A
pSLQ5428_pHR_EF1a-mCherry-P2A-Rfx_Cas13d-2xNLS-3xFLAG	Abbott et al.[2]	N/A
*pSLQ5429_pUC_hU6-crScaffold_EF1a-BFP	Abbott et al.[2]	N/A
*pSLQ5465_pHR_hU6-crScaffold_EF1a-PuroRT2A-BFP	Abbott et al.[2]	N/A
*Denotes generic backbone plasmid for crRNAs. Specific target sequences for crRNAs can be found in Table S2.	Abbott et al.[2]	N/A
Software and algorithms		
Cytobank	Beckman Coulter	N/A
FlowJo v10	https://www.flowjo.com/	N/A
Geneious 2020.0.4	https://www.geneious.com	N/A
MAFFT	Nakamura et al.[39]	https://mafft.cbrc.jp/alignment/software/
Bowtie	Langmead et al.[40]	http://bowtie-bio.sourceforge.net/index.shtml
Bowtie 2	Langmead et al.[41]	http://bowtie-bio.sourceforge.net/bowtie2/index.shtml
iTOL v5.5	Letunic and Bork[18]	https://itol.embl.de/
Cas13 Guide RNA Design	Wessels et al.[14]	https://gitlab.com/sanjanalab/cas13
CRISPR-PACMAN crRNA design tool	This paper	https://github.com/QilabGitHub/CRISPR-PACMAN-pool-generation

RESOURCE AVAILABILITY

Lead contact

Further information and requests for resources and reagents should be directed to and will be fulfilled by the lead contact, Lei S. Qi (stanley.qi@stanford.edu).

Materials availability

All materials and reagents will be made available upon installment of a material transfer agreement (MTA). All plasmids will be available from Addgene (https://www.addgene.org/Stanley_Qi/).

Data and code availability

The codes for CRISPR-PACMAN computational pipeline are deposited in GitHub (https://github.com/QilabGitHub/CRISPR-PACMAN-pool-generation). Additional Supplemental Items are available from Mendeley Data at https://dx.doi.org/10.17632/bgxfwsg3sb.1

EXPERIMENTAL MODEL AND SUBJECT DETAILS

Cell culture

All cell lines were incubated at 37°C and at 5% CO_2. Human embryonic kidney (HEK293T) cells and A549 cells (ATCC CCL-185) were cultured in 10% fetal bovine serum (Thermo Fisher Scientific) in DMEM (Thermo Fisher Scientific).

METHOD DETAILS

A general pipeline for crRNA analysis

All RNA virus genomes were retrieved from public databases, including 16 RNA virus families from the Virus Pathogen Database and Analysis Resource (ViPR), human immunodeficiency virus (HIV) from NCBI, and IAV from the Influenza Research Database (IRD) (Table S1).

The viral genomes are aligned by Multiple Alignment using Fast Fourier Transform[39] (MAFFT) and a 22-nucleotide (nt) sliding window is passed over the alignment. In each window, if there is a 22-nt sequence with no gap characters that appears in > 50% of genomes then that sequence is added to the crRNA set. In order to eliminate crRNAs with off-targets in the human genome, Bowtie[40] is used to identify crRNAs that align to the human transcriptome with $\leq$ 2 mismatches; these crRNAs as well as crRNAs with the poly-U (> = 4U's) sequence that may prevent crRNA expression are removed from the guide set. All crRNAs are assigned a predicted efficiency score based on Wessels et al.[14] Cas13 guide design method as described in the paragraph below.

To assign each crRNA with a predicted efficiency score, we utilized a recently published computational tool that generates Cas13 crRNAs and predicted efficiency scores given a single input sequence.[14] First, for each viral group we choose a representative sequence, which is a NCBI reference sequence if one exists in the viral group, or a random sequence from the viral group. We use the Cas13 Guide Design Tool[14] to generate crRNAs against this reference sequence. Because all CRISPR-PACMAN crRNAs are 22nt, in contrast to the 23nt crRNAs generated by the tool, we assign each crRNA the average score of all output crRNAs of which it is a substring.

Species-specific crRNAs refer to those crRNAs that target conserved regions in a group of closely related viral genomes. The viruses in a group can be members of the same viral genus (e.g., betacoronaviruses) and pathogenic species (e.g., SARS-CoV-2 patient isolates). In species-specific crRNAs, we also identify and label crRNAs which target other viral genus or other pathogenic species in the same family.

The minipool of family-covering crRNAs is determined through an iterative process. The crRNAs are ranked by the number of unique genomes they appear in and the crRNA that targets the most genomes is added to the list. The process is repeated, and the crRNAs are ranked by the number of unique genomes that are not already targeted. If multiple crRNAs are tied in a step, the crRNA with the fewest 3-mer repeats (e.g., "AAA" or "GGG") is selected. The process ends when every virus strain in the family is targeted by at least one crRNA in the list. Note that the ordering of crRNAs in the list is significant; necessarily, the first crRNA in the list will target the largest number of virus strains.

Format of dataset in CRISPR-PAC-MAN server

The downloadable file format of crRNAs is a TSV file, in which each crRNA is annotated with its genomic sequence, spacer DNA for synthesis, % GC content, and additional features. The TSV file for the species-specific crRNAs has an additional column, "Specific to group," to demonstrate whether the guide is specific to the group (i.e., no alignments with zero mismatches to any sequence in other groups in the same viral family, as determined by Bowtie2[41]). Minipool crRNAs are annotated by the cumulative percentage of sequences in the virus family that can be targeted by this crRNA and preceding crRNAs in the list. The cumulative percentage of sequences targeted by the last crRNA in the list will be 100%. Users can click on coding sequences of interest to selectively download

guides targeting those regions. We include a link to the iTOL website for each phylogenetic tree to enable users to interact with the tree. A tutorial video is available at the permanent link: https://www.youtube.com/watch?v=S2sPLE7i_6k.

SARS-CoV-2 targeting in CRISPR-PACMAN

A focused webpage was developed for users to access crRNAs targeting SARS-CoV-2 and the coronavirus family (Figures 3A–3C; http://crispr-pacman.stanford.edu/sarscov2). This webpage hosts: 1) species-specific crRNAs targeting conserved regions of SARS-CoV-2, 2) a coronavirus-covering crRNA minipool that collectively target all sequenced coronaviruses, and 3) custom crRNAs that can target both SARS-CoV-2 and another virus species, such as SARS-Cov or MERS-CoV. Because new sequences of SARS-CoV-2 patient isolates are frequently released, these crRNA sets are frequently updated. This page also highlights experimental validation data for SARS-CoV-2 crRNAs.

Our previous study developed a set of crRNAs to target highly conserved regions among the SARS-CoV-2, SARS-CoV and MERS-CoV genomes.[2] These crRNAs are featured as a track on the UCSC Genome Browser,[17] which is linked to the SARS-CoV-2 resource page. We characterized each crRNA on the UCSC Genome Browser with relevant features, including predicted efficiency score, reported off-target loci, percentage of SARS-CoV-2 targeted, and percentage of coronaviruses targeted.

Design and cloning of RdRP- and N-targeting crRNAs

The crRNA plasmids were cloned using standard restriction-ligation cloning. Forward and reverse oligos for each spacer (IDT) were annealed and inserted into the backbone using T4 DNA Ligase (NEB). Assembled oligos were either inserted into a pHR backbone, obtained and modified from Addgene (#121514 and #109054, respectively). Spacer sequences for all crRNAs can be found in Table S2.

Design and cloning of SARS-CoV-2 reporters

To clone SARS-CoV-2 reporters, pHR-PGK-scFv GCN4-sfGFP (pSLQ1711) was digested with EcoR1 and Sbf1 and gel purified. The PGK promoter and sfGFP were PCR amplified from pSLQ1711 and gel purified. The SARS-CoV-2-F1 and SARS-CoV-2-F2 fragments were synthesized from Integrated DNA Technologies (IDT). At last, the PGK, sfGFP, and SARS-CoV-2-F1/F2 fragments were inserted into the linearized pSLQ1711 vector using In-Fusion cloning (Takara Bio).

Lentiviral packaging and cell line generation

On day 1, HEK293T cells were seeded into 100mm dishes (Corning). On day 2, cells were ~50%–70% confluent at the time of transfection. For each dish, 6 μg of pHR vector containing the construct of interest, 4 μg of dR8.91 and 1 μg of pMD2.G (Addgene) were mixed in 1 mL of Opti-MEM reduced serum media (GIBCO) with 30 μL of Mirus TransIT-LT1 reagent and incubated at room temperature for 30 minutes. The transfection complex solution was distributed evenly to HEK293T cultures dropwise. On day 5, lentiviruses are harvested from the supernatant with a sterile syringe and filtered through a 0.22-μm polyvinylidene fluoride filter (Millipore).

For A549 cells, lentivirus precipitation solution (Alstem) was added and precipitated as per the manufacturer's protocol. One well of a 6-well plate (Corning) of A549 cells at ~50% confluency was transduced with the precipitated lentivirus. After 2-3 days of growth, the cell supernatant containing the virus was removed and the cells were expanded. Cells were then sorted for mCherry+ cells using a Sony SH800S cell sorter.

SARS-CoV-2 reporter challenge experiments

On day 1, A549 cells stably expressing Cas13d (hereafter referred to as Cas13d A549) were seeded at a density of 80,000 cells per well in a 12-well plate. On day 2, Cas13d A549 cells were transfected with crRNAs targeting the two SARS-CoV-2 reporters or a non-targeting crRNA along with the respective SARS-CoV-2 reporters in an equimolar ratio using Mirus LT1 reagent (100 μL Opti-MEM reduced serum media, 0.5 μg crRNA, 1 μg SARS-CoV-2 reporter, 4 μL Mirus LT1 per well). Wild-type cells were transfected with either the crRNA or SARS-CoV-2 reporter plasmids as compensation controls. GFP expression was measured on day 4 by flow cytometry on a Beckman-Coulter CytoFLEX S instrument. Data was analyzed using FlowJo v10. All p values are available in Table S3.

Quantitative RT-PCR (qRT-PCR)

Real-time qRT-PCR was performed to quantify RNA abundance. For each sample, total RNA was isolated by using the RNeasy Plus Mini Kit (QIAGEN Cat# 74134), followed by cDNA synthesis using the iScript cDNA Synthesis Kit (BioRad, Cat# 1708890). qRT-PCR primers were ordered from Integrated DNA Technologies (IDT). Quantitative PCR was performed using the PrimePCR assay with the SYBR Green Master Mix (BioRad) and run on a Biorad CFX384 real-time system (C1000 Touch Thermal Cycler), according to manufacturers' instructions. Cq values were used to quantify RNA abundance. The relative abundance of the SARS-CoV-2 fragments was normalized to a GAPDH internal control. Primers used in qPCR are available in Table S4.

QUANTIFICATION AND STATISTICAL ANALYSIS

Flow cytometry

For quantification of repression efficiency by flow cytometry (Figure 4A), values represent mean of fluorescence signals in GFP positive cells. Statistical analyses were performed using a two-sided t test with unequal variance in Excel to calculate p values (Table S3).

Quantitative RT-PCR (qRT-PCR)

For quantification of RNA abundance by qRT-PCR (Figures 4B and S3C), the relative RNA expression of the SARS-CoV-2 fragments was normalized to a GAPDH internal control. To calculate the relative mRNA abundance, the relative RNA expression of each treatment was normalized by setting the average value in reporter only samples as 1. Statistical analyses were performed using a two-sided t test with unequal variance in Excel to calculate p values (Table S3).

Cell Reports Medicine, Volume *2*

Supplemental information

A comprehensive analysis and resource to use CRISPR-Cas13 for broad-spectrum targeting of RNA viruses

Xueqiu Lin, Yanxia Liu, Augustine Chemparathy, Tara Pande, Marie La Russa, and Lei S. Qi

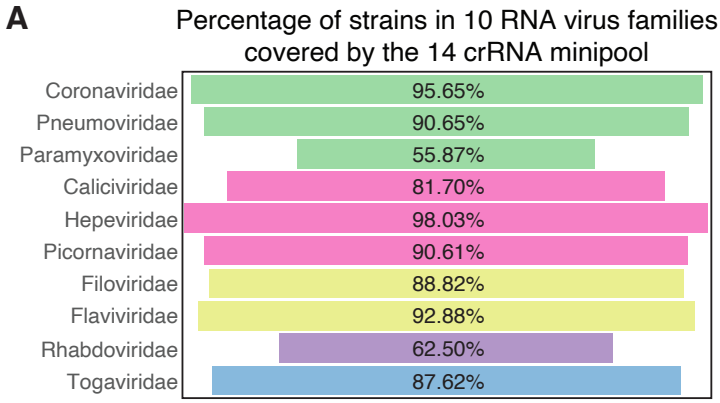

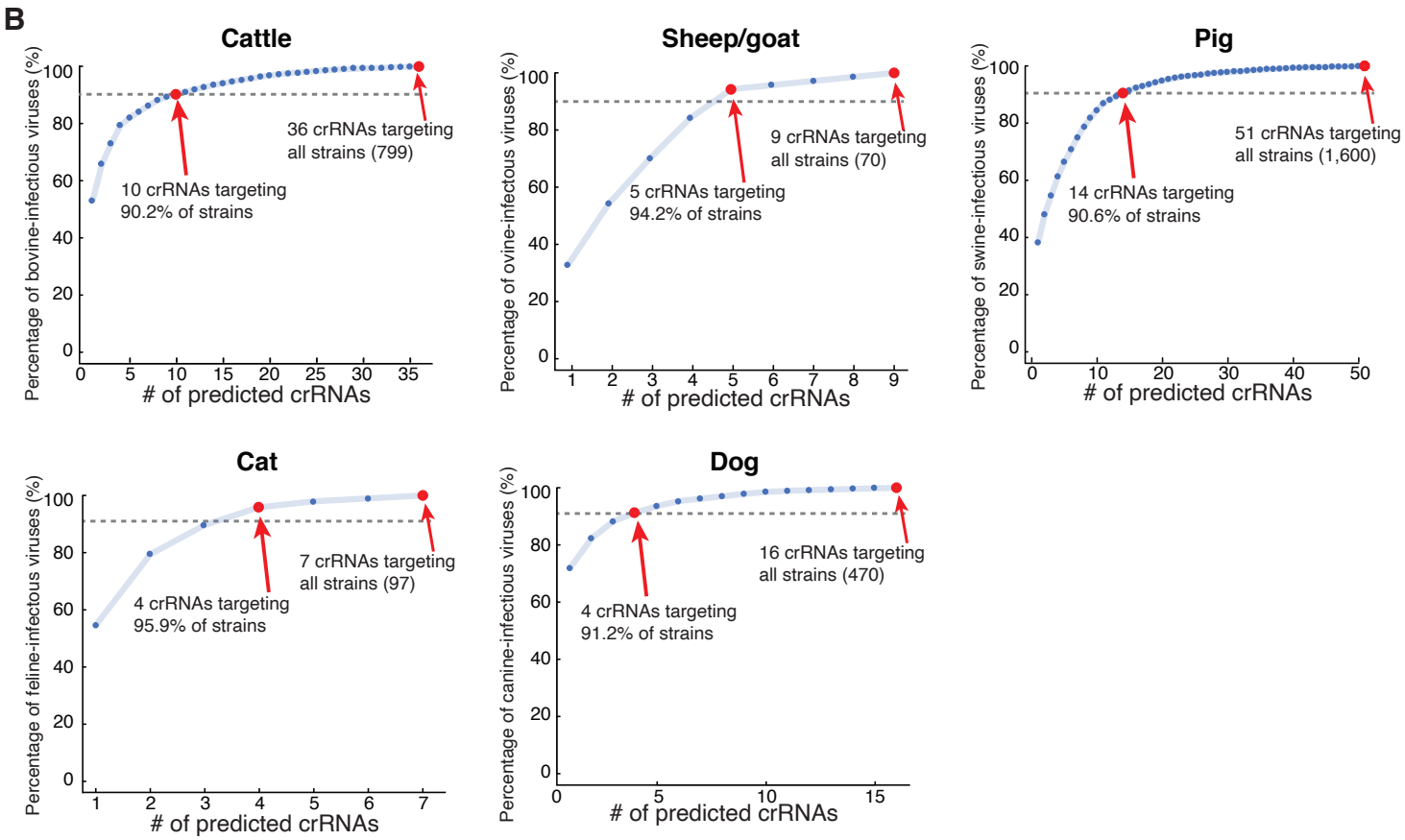

Figure S1. Analysis of crRNAs targeting broad-spectrum RNA viruses. Related to Figure 1.

A. Coverage of human-infectious strains in each of 10 RNA virus families by 14 minipool crRNAs.
B. Cumulative curves showing the predicted number of minipool crRNAs to target animal-infectious strains in 10 RNA virus families.

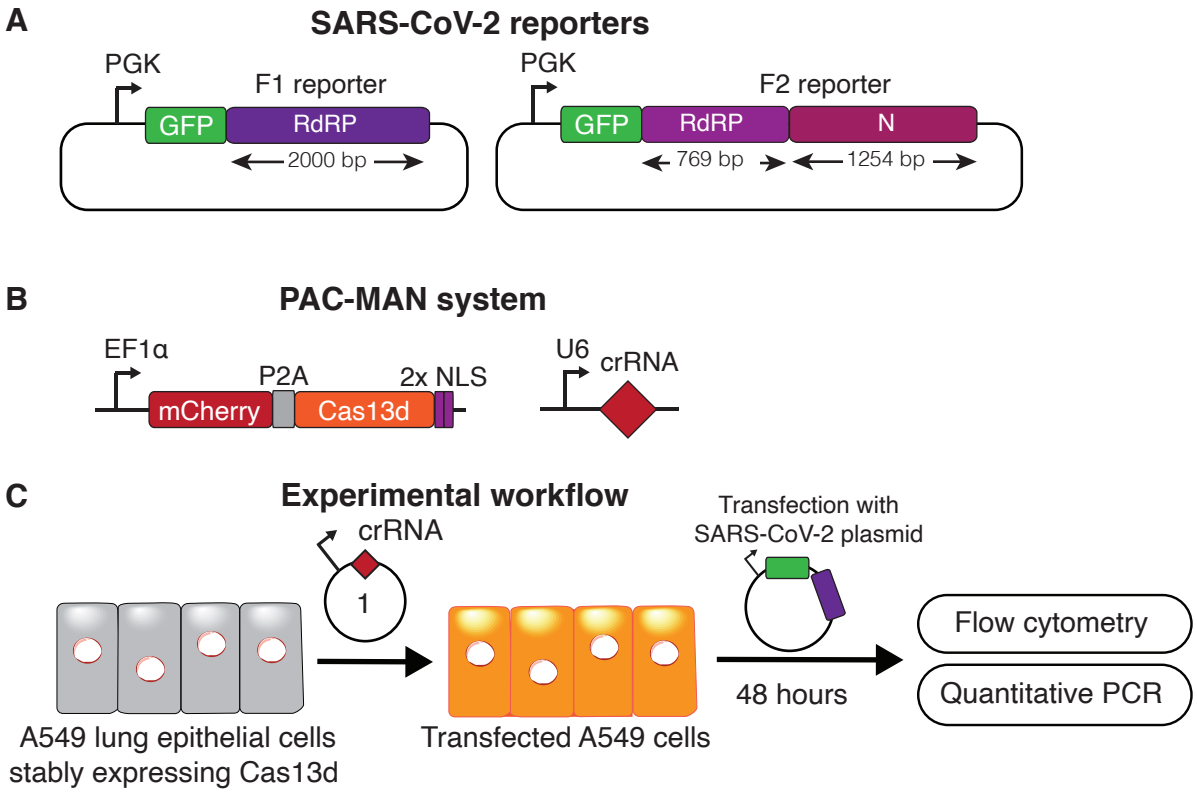

Figure S2. Schematics of experimental systems and workflow used to validate crRNAs. Related to Figure 4.

A. The SARS-CoV-2 reporters used in this study.
B. PAC-MAN expression system used in this study.
C. Workflow for quantifying all individual or combinatorial crRNAs for targeting SARS-CoV-2 sequences.

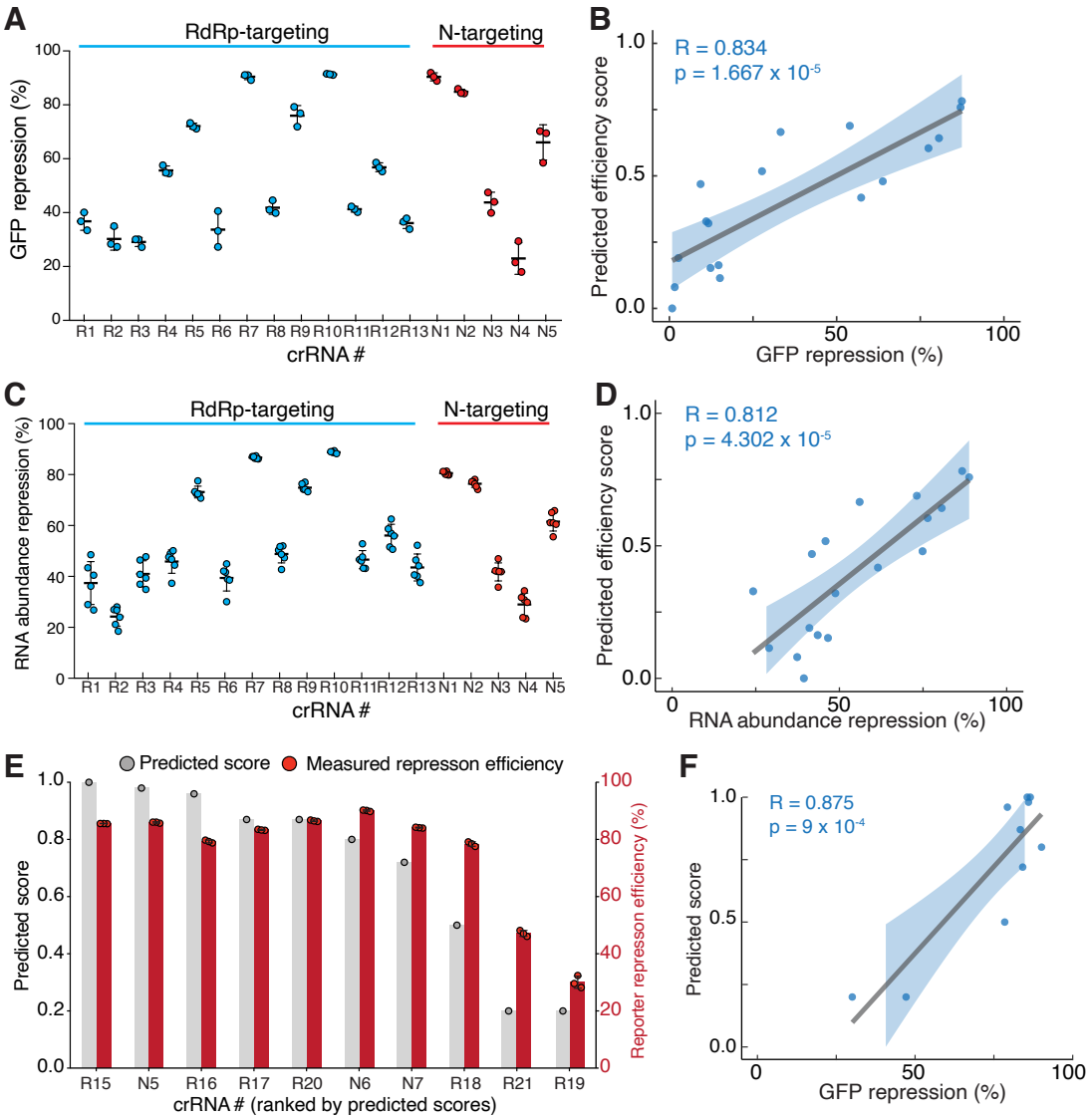

Figure S3. Validation of predicted crRNAs for targeting SARS-CoV-2 sequences. Related to Figure 4.

A. Repression on SARS-CoV-2 GFP reporter using the first batch of crRNAs measured by flow cytometry. p values related to reporter only samples for each group are included in Table S3. Lines indicate means; error bars indicate s.d. (n = 3 independent biological replicates).

B. Correlation between predicted efficiency score and SARS-CoV-2 GFP repression efficiency for the first batch of crRNAs.

C. Repression on SARS-CoV-2 reporter RNA abundance using the first batch of crRNAs measured by qPCR. RNA abundance is calculated by normalizing to the reporter only sample. p values related to reporter only samples for each group are included in Table S3. Lines indicate means; error bars indicate s.d. The data represent three independent biological experiments performed in technical replicates (n = 6).

D. Correlation between predicted efficiency score and RNA abundance repression efficiency for the first batch of crRNAs.

E. Comparison of repression on SARS-CoV-2 GFP reporter (red) and predicted efficiency scores (grey) using the second batch of crRNAs. p values related to reporter only samples for each group are included in Table S3. Lines indicate means; error bars indicate s.d. (n = 3 independent biological replicates).

F. Correlation between predicted efficiency score and SARS-CoV-2 GFP repression efficiency for the second batch of crRNAs.